Stability of the parallel flow of a fluid over a slightly heavier fluid

By ROBIN E. ESCH

Computation Laboratory, Harvard University

(Received 26 February 1960 and in revised form 10 July 1961)

The incompressible, inviscid, parallel flow of a layer of fluid over a slightly denser fluid, in the presence of gravity, is investigated for stability. Two idealized piecewise-linear steady velocity profiles are examined analytically, and a comparison with related experimental results is made.

The dimensionless parameter $U/(gh)^{\frac{1}{2}}$, where U is flow velocity, g the acceleration of gravity, and h the thickness of the upper layer, appears to have a critical value between 0·2 and 0·7, below which stable flows can persist. At the onset of instability disturbances of wavelength about h or $2h$ are predicted, with more violent disturbances of longer wavelength occurring at higher values of $U/(gh)^{\frac{1}{2}}$. For continuous steady velocity profiles this instability phenomenon is found to be relatively insensitive to the ratio of the densities of the two fluids.

1. Introduction

Certain interesting and important physical situations involve the flow of a stream of fluid through a larger body of fluid. An example is the flow of a river into an estuary. Here the slightly higher density of salt water in the estuary tends to make the fresh river water remain on top. Another example is the flow of organic or radioactive wastes through a detainer tank. If dead regions of fluid form in such a tank, its effective size can be much reduced, with unfortunate consequences. Other oceanographic or meteorological examples can be found.

The detailed motion in such situations is usually complex. However, two opposite types of behaviour can be distinguished: either the fluid all mixes up together in a turbulent manner, or a motionless region of fluid is observed, past which the fluid flows in a stream.

The classical mathematical approach to such problems is of course parallel-flow stability analysis, discussed at length by Lin (1955), and perhaps first employed by Rayleigh (1945, pp. 385 *et seq.*) and Helmholtz (see Lamb 1945, pp. 373 *et seq.*). This approach postulates a steady (i.e. time-independent) parallel flow, and determines whether or not superimposed infinitesimal time-dependent disturbances can grow.

Following this technique, we might attempt to gain insight into the physical situations of interest by considering the following already much idealized two-dimensional problem, as indicated in figure 1 (*a*).

Gravity acts in the $-y$-direction. An air-water interface occurs at $y = h$,

and another interface between two regions of water of slightly different densities occurs at $y = 0$, the higher density being below, so that

$$\text{density} = \begin{cases} 0 & y > h, \\ \rho_a & 0 < y < h, \\ \rho_b & y < 0, \end{cases}$$

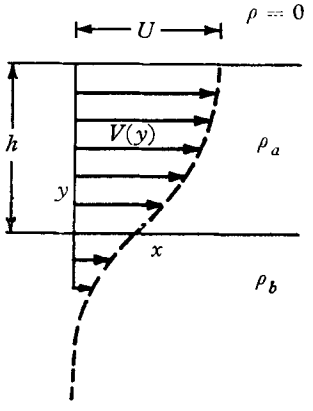

FIGURE 1*a*. Physically possible steady flow profile.

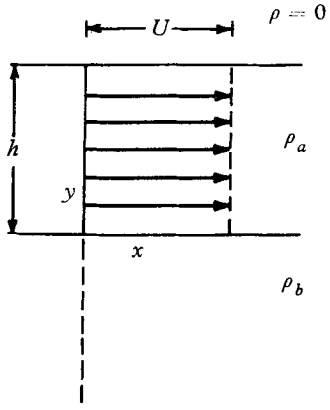

FIGURE 1*b*. Discontinuous profile.

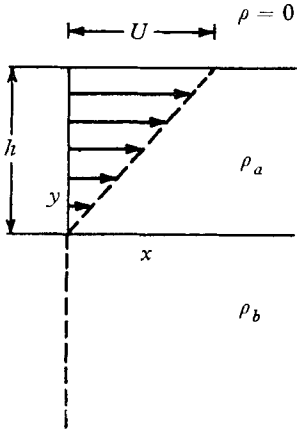

FIGURE 1*c*. Shear-layer profile.

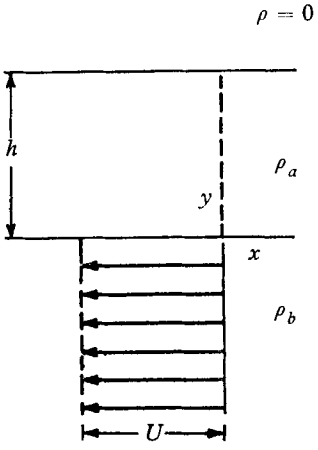

FIGURE 1*d*. Discontinuous profile.

where ρ_a/ρ_b is slightly less than unity. A steady current in the x-direction, given by $V(y)$ and with magnitude characterized by U, is present as pictured in figure 1 (*a*).

An infinitesimal 'disturbance' velocity field $[u(x, y, t), v(x, y, t), 0]$ is assumed to be superimposed on this steady flow field. The infinitesimal velocity components u and v are assumed to be of the form $f(y)\, e^{i\alpha(x-ct)}$. The stability analysis would now consist of determining c, and noting under what conditions its imaginary part is positive, corresponding to a growing infinitesimal disturbance. Ideally we should also investigate the completeness of the resulting set of disturbance

modes, and verify that any disturbance modes not included in the analysis can legitimately be ignored in stability considerations; physical arguments, and experimental and theoretical results in similar problems, seem to indicate that this is indeed the case (Lin 1955).

The quantity c, which plays the role of an eigenvalue, is a function of the parameters of the problem h, U and ρ_b/ρ_a, and of the disturbance wave-number α. The important physical mechanisms of the problem are: (i) the strong stabilizing influence of the large density change at the upper interface; (ii) the weak stabilizing influence of the small density change at the lower interface; (iii) the destabilizing influence of the shearing parallel flow, which results in the phenomenon called Helmholtz instability.

Previous investigations (Esch 1957) indicated that (in contrast to the situation with solidly bounded flows) in stability analysis of a parallel flow where solid boundaries are effectively absent, inviscid-theory results apply to a good degree of approximation down to fairly small Reynolds number, the major effect of viscosity above this Reynolds number being through its influence on the velocity profile of a possible steady flow. (Specifically, this was found to be true for αR greater than about 100, where R is a Reynolds number and α a dimensionless disturbance wave-number.) Furthermore, stability results were found to be insensitive to minor changes in the velocity profile, when the wavelength of important disturbance modes is long compared to the extent of the region in which change is made.

With this encouragement, further severe simplifications were made which reduce the problem to one which is readily soluble. It was hoped that the essential physical mechanisms were retained, so that some conclusions could be drawn about the more realistic problem pictured in figure 1 (*a*). Viscosity was neglected throughout. First the *discontinuous profile* shown in figure 1 (*b*) was treated; this is the type of flow originally considered by Helmholtz (see Lamb 1945, p. 373), complicated by having unequal densities on either side of the lower interface, and by the presence of the upper interface. The discontinuity in tangential velocity is of course objectionable on physical grounds, and leads to unrealistic mathematical results at large disturbance wave-numbers. (It was more convenient for algebraic reasons to treat the profile of figure 1 (*d*), which is physically the same as that of figure 1 (*b*), being the same flow viewed from a moving co-ordinate system; this merely results in shifting the eigenvalues c by an additive real constant.) Secondly, the physically more reasonable profile shown in figure 1 (*c*) was treated; this profile will be called the *shear-layer profile*.

Bjerknes, Bjerknes, Solberg & Bergeron (1933, article 107) have derived the eigenvalue equation for the discontinuous profile, without extracting roots. Godske, Bergeron, Bjerknes & Bundgaard (1957, chapter 10) further discuss models of this type, in the context of meteorology. Goldstein (1931) and Taylor (1931), and more recently Drazin (1958) and Menkes (1959), have investigated related problems involving shear layers between unbounded flows, with vertical variation of density; the problem considered here differs through the presence of the strongly stable upper free surface.

2. Discontinuous profile calculations and results

The parameters h and U will be used as reference length and velocity; thus, now indicating dimensional variables by asterisks, we define dimensionless variables as follows:

$$\left.\begin{aligned} x &= x^*/h, & V &= V^*/U, \\ u &= u^*/U, & \rho &= \rho^*/\rho_0, \\ t &= (U/h)\,t^*, & p &= p^*/(\rho_0 U^2). \end{aligned}\right\} \tag{1}$$

An arbitrary reference density ρ_0 has also been introduced, for future convenience. The driving mechanism will enter the problem through the dimensionless parameter

$$G = gh/U^2. \tag{1'}$$

Within any region where viscosity is negligible, flow is irrotational, so that a scalar velocity potential ϕ exists, density is constant, and the only body force is gravity acting in the negative y-direction; the fluid equations may then be written

$$\left.\begin{aligned} (u, v, w) &= (\phi_{,x};\ \phi_{,y};\ \phi_{,z}), \\ \nabla^2\phi &= 0, \\ p = \text{const.} - \rho G y - \tfrac{1}{2}\rho(u^2+v^2+w^2) &- \rho\phi_{,t}, \end{aligned}\right\} \tag{2}$$

where subscripts have been used to indicate partial differentiation.

The first problem considered is that of small two-dimensional disturbances superimposed on the discontinuous steady-flow profile pictured in figure 1 (*d*). Region a (i.e. the region $0 < y < 1$; a for *above*) has constant density $\rho_a = 1$, region b ($y < 0$; b for *below*) has constant density ρ_b, and the region $y > 1$ has negligibly small density. In the absence of disturbances, the fluid in region a is at rest, while that in region b is moving to the left with constant velocity unity.

If ϕ_a and ϕ_b denote the velocity potentials in regions a and b, and $y = \eta(x,t)$ and $y = 1+\xi(x,t)$ the equations of lower and upper interfaces, where η and ξ are the result of small disturbances, and if sinusoidal x-dependence is assumed, it is found that

$$\left.\begin{aligned} \phi_a &= \{a_1 e^{\alpha y} + a_2 e^{-\alpha y}\}\, e^{i\alpha(x-ct)}, \\ \phi_b &= -x + a_3 e^{\alpha y}\, e^{i\alpha(x-ct)}, \\ \eta &= a_4 e^{i\alpha(x-ct)}, \\ \xi &= a_5 e^{i\alpha(x-ct)}, \end{aligned}\right\} \tag{3}$$

where ϕ_a and ϕ_b have already been required to obey Laplace's equation, and ϕ_b has been required to remain bounded as $y \to -\infty$. The constants $a_1, a_2, \ldots, a_5$ are assumed to be small. The parameter α is the wave-number of the disturbance, $\mathrm{Re}\,(c)$ the phase velocity, and $\alpha\,\mathrm{Im}\,(c)$ the growth rate. A disturbance grows, decays or remains of the same magnitude according as $\mathrm{Im}\,(c)$ is found to be greater than 0, less than 0, or equal to 0.

The conditions that remain to be satisfied are continuity of pressure and normal velocity at the interfaces, and compatibility between the interface equations

and the velocity potentials. If we neglect second and higher powers of small quantities, these conditions yield the equations

$$\left.\begin{aligned} \eta_{,t}-\eta_{,x} &= \phi_{b,y}|_{y=0}, \\ \eta_{,t} &= \phi_{a,y}|_{y=0}, \\ \xi_{,t} &= \phi_{a,y}|_{y=1}, \\ p_a(\eta) &= p_b(\eta), \\ p_a(1+\xi) &= \text{const.} \end{aligned}\right\} \tag{4}$$

Substituting equations (2) and (3) into equations (4) and again neglecting higher-order terms, we have

$$\left.\begin{aligned} a_3+i(c+1)\,a_4 &= 0, \\ a_1-a_2+ica_4 &= 0, \\ e^{\alpha}a_1-e^{-\alpha}a_2+ica_5 &= 0, \\ i\alpha ca_1+i\alpha ca_2-i\alpha\rho_b(c+1)\,a_3+(\rho_b-1)\,Ga_4 &= 0, \\ i\alpha ce^{\alpha}a_1+i\alpha ce^{-\alpha}a_2-Ga_5 &= 0, \end{aligned}\right\} \tag{5}$$

which are 5 linear homogeneous equations in a_1, a_2, a_3, a_4, a_5. The condition for a non-trivial solution is that the determinant be zero, which yields the eigenvalue equation

$$\left[c^2-\frac{G}{\alpha}\right]\left[(\rho_b+1)\,c^2+2\rho_b c+\rho_b-\frac{(\rho_b-1)}{\alpha}G\right] + e^{-2\alpha}\left[c^2+\frac{G}{\alpha}\right]\left[(\rho_b-1)\,c^2+2\rho_b c+\rho_b-\frac{(\rho_b-1)}{\alpha}G\right]=0. \tag{6}$$

The roots of this quartic in c are the desired eigenvalues. An obvious approach for large values of α is to use a perturbation series in $e^{-2\alpha}$, whereby the expansion

$$c = c_0+c_2e^{-2\alpha}+c_4e^{-4\alpha}+\ldots \tag{7}$$

is substituted into (6) and coefficients of like powers of $e^{-2\alpha}$ are equated to zero in order to evaluate c_0, c_2, etc. The leading coefficient c_0 is found (by merely omitting the second term in (6)) to be

$$c_0 = \pm\left(\frac{1}{\alpha}\frac{gh}{U^2}\right)^{\frac{1}{2}}, \quad (\rho_b+1)^{-1}\left\{-\rho_b\pm\left[\frac{1}{\alpha}\frac{gh}{U^2}(\rho_b^2-1)-\rho_b\right]^{\frac{1}{2}}\right\}. \tag{8}$$

The root of interest is of course the one with positive imaginary part:

$$c_0 = (\rho_b+1)^{-1}\left\{-\rho_b+i\left[\rho_b-\frac{1}{\alpha}\frac{gh}{U^2}(\rho_b^2-1)\right]^{\frac{1}{2}}\right\}. \tag{8'}$$

The next step yields

$$= \frac{-\left[c_0^2+\frac{G}{\alpha}\right]\left[(\rho_b-1)\,c_0^2+2\rho_b c_0+\rho_b-(\rho_b-1)\frac{G}{\alpha}\right]}{2c_0\left[(\rho_b+1)\,c_0^2+2\rho_b c_0+\rho_b-(\rho_b-1)\frac{G}{\alpha}\right]+\left(c_0^2-\frac{G}{\alpha}\right)[2c_0(\rho_b+1)+2\rho_b]}. \tag{9}$$

The approximation $c_0+c_2e^{-2\alpha}$ was found to give good accuracy for all $\alpha > 1$.

For smaller values of α, numerical methods were used to obtain solutions of the eigenvalue equation. Both the quadratic factor method and the complex Birge–Vieta method (Kunz 1957) were tried, and found to be equally satisfactory and equally simple to programme for machine solution. In both methods minor inconvenience was caused by the difficulty of finding initial approximations sufficiently accurate for the iterative method to converge, when operating in the immediate neighbourhood of a double root; however, simple and crude provisions in the programme easily cope with such difficulties.

Because of the nature of the physical problems of interest, consideration was limited to density ratios in the range

$$1{\cdot}00 \leqslant \rho_b \leqslant 1{\cdot}06.$$

For ρ_b in this range, (6) was found to have either 4 real roots, or 2 real roots and a complex conjugate pair of roots. Thus at most one of the four disturbance modes is unstable (i.e. has $\operatorname{Im} c > 0$). The major result is shown on figure 2 (*a*), where the horizontal co-ordinate is α and the vertical co-ordinate $G^{-\frac{1}{2}} = U/(gh)^{\frac{1}{2}}$ (chosen because it is directly proportional to U). The relevant curves are labelled 'discontinuous profile'; these are neutral stability curves, and are loci of double roots of (6), which has only real roots in the region below. Thus unstable disturbance modes exist only at points above these curves. Curves are given for three typical density ratios $\rho_b/\rho_a = 1{\cdot}06$, $1{\cdot}04$ and $1{\cdot}02$, and are seen to become lower as the density ratio decreases. The neutral stability curve for $\rho_b/\rho_a = 1{\cdot}00$ is simply the horizontal axis, i.e. an unstable disturbance mode then exists for any pair of values (α, G).

Now physically a problem is characterized by the two parameters G and ρ_b/ρ_a; an initial value problem must be solved by Fourier synthesis, i.e. by superposing appropriate amounts of the four modes for various values of wave-number α. In practice it must be assumed that small disturbances of all wavelengths are present. Thus we see from figure 2 (*a*) that the discontinuous profile is physically unstable for any U, due to the unlimited instability at high wave-numbers α, a well-known property of Helmholtz instability of flow profiles which have discontinuities. This objectionable feature is not found in the next model considered (figure 1 (*c*)), where the distributed shear provides a mechanism for stabilizing the situation at high wave-numbers.

In every unstable case, the value of $\operatorname{Re}(c)$ was found to imply that the disturbance had phase velocity between 0 and U, in the direction of the steady flow. The disturbance does not have a travelling wave character, but is convected at some velocity intermediate between the velocities of the streams above and below the interface at $y = 0$. (This remark also applies to the calculations for the shear-layer profile, figure 1 (*c*), discussed later.)

It is of some interest to look at the effect of varying the layer thickness h, while holding other physical parameters constant. Some trivial manipulation is required, since h has been used freely in putting the problem into dimensionless form. We wish now to hold U, and dimensional wave-number α/h constant (therefore α will vary in proportion to h), and look at the dimensional growth rate $(\alpha U/h) \operatorname{Im} c$, as we vary h. We desire a plot of results in which the effect of

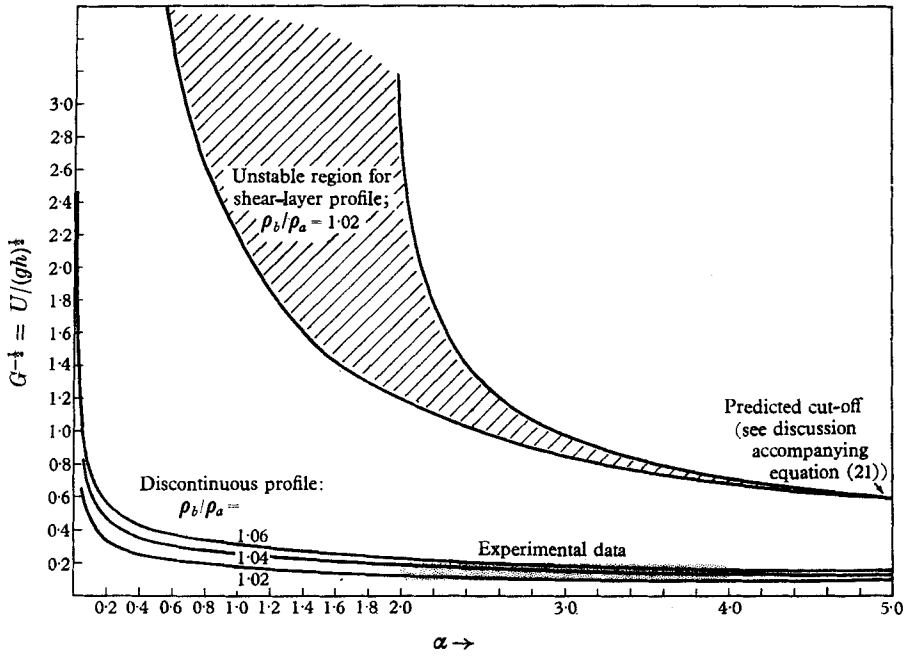

FIGURE 2*a*. Neutral stability curves. The regions of instability are: for the discontinuous profile, everywhere above the neutral stability curve; for the shear-layer profile, only the cross-hatched region. In the dotted region onset of instability in a flume was observed, with density ratios in the range $1{\cdot}00 < \rho_b/\rho_a < 1{\cdot}01$.

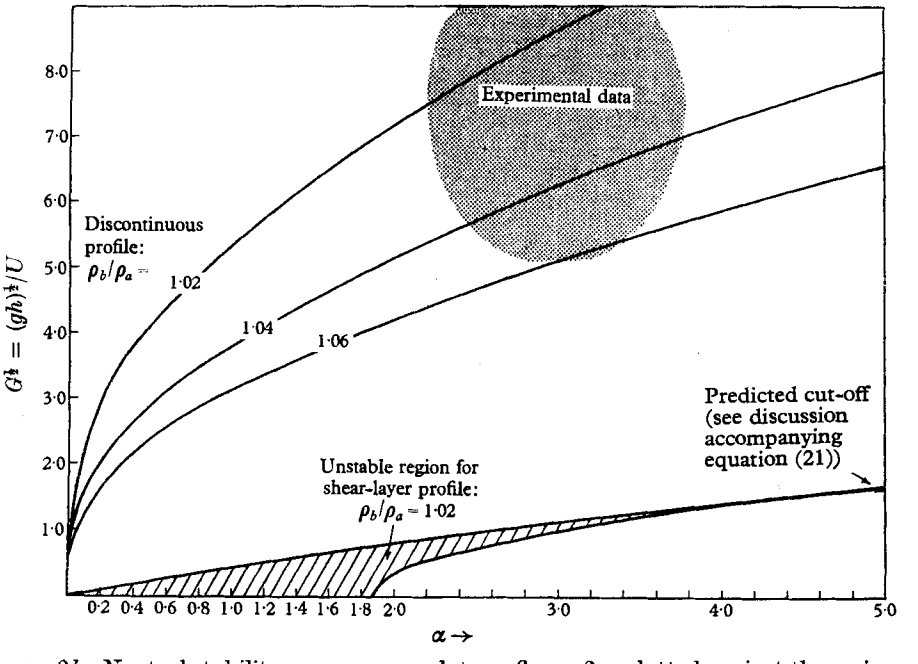

FIGURE 2*b*. Neutral stability curves: same data as figure 2*a*, plotted against the reciprocal ordinate $G^{\frac{1}{2}} = (gh)^{\frac{1}{2}}/U$. The regions of instability are: for the discontinuous profile, everywhere below the neutral stability curve; for the shear-layer profile, only the cross-hatched region.

varying h is isolated in the horizontal co-ordinate α (to which it is proportional in the process described above). Therefore we choose as vertical co-ordinate the forcing parameter

$$\theta = \left(\alpha \frac{U^2}{gh}\right)^{\frac{1}{2}} = (\alpha/G)^{\frac{1}{2}} \tag{10}$$

and plot lines of constant $\operatorname{Im} \phi$, a dimensionless growth rate given by the imaginary part of

$$\phi = \left(\frac{h}{\alpha g}\right)^{\frac{1}{2}} \left[\frac{\alpha U}{h} c\right] = \theta c, \tag{11}$$

because θ and ϕ remain constant when h is varied in the manner described above, and $\operatorname{Im} \phi$ is just a dimensional constant times the dimensional growth rate.

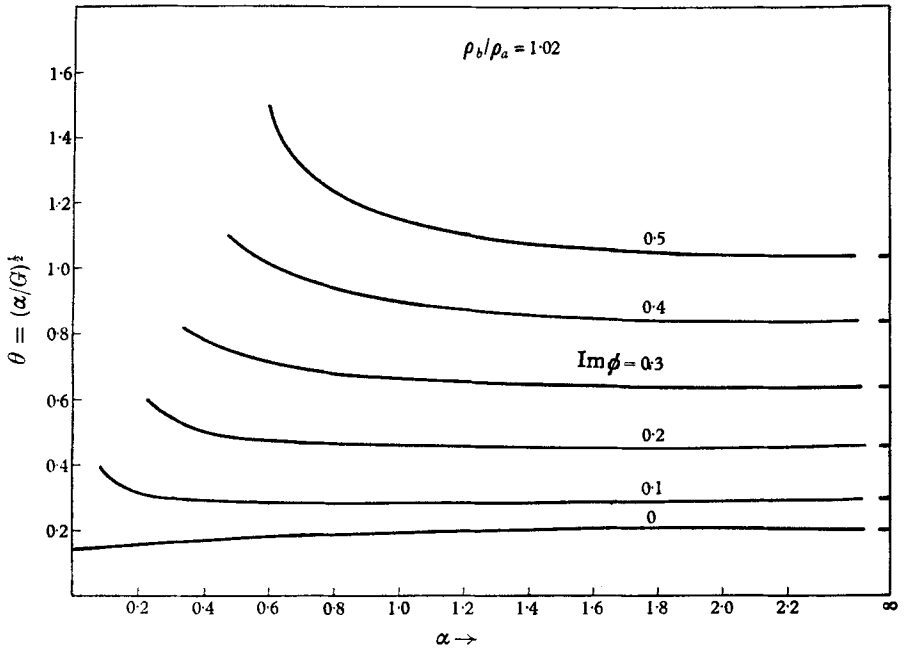

FIGURE 3. Constant growth-rate curves for the discontinuous profile with $\rho_b/\rho_a = 1{\cdot}02$.

The results are shown in figure 3, for the typical density ratio $\rho_b/\rho_a = 1{\cdot}02$. At large α, exponentially small terms in the eigenvalue equation can be neglected, and the result factors into two quadratics, with roots given by (8). This reflects the physical fact that at large α the wavelength $2\pi h/\alpha$ is much less than the layer thickness h, and the two interfaces do not interact appreciably. The first pair of roots in (8) correspond to surface waves at the upper interface, which die out in a few wavelengths away from the interface. The second pair correspond to a disturbance centred about the lower interface, which has a wave character if $(\rho_b^2 - 1) > \theta^2 \rho_b$, and otherwise a growing character. This is simply the classical Helmholtz instability situation for the interface between two fluids of unlimited extent.

As α is reduced from large values, the unstable mode will begin to involve appreciable motion at the upper interface. This might be expected on physical

grounds to have a stabilizing influence, and we see from figure 3 that this is indeed true, since the $\mathrm{Im}\,\phi = \text{const.}$ lines rise as α is reduced. The anomalous lowering of the $\mathrm{Im}\,\phi = 0$ (neutral stability) curve is not explained by this physical argument.†

At small h ascending power series in α are of interest. Again it is appropriate to replace c and G/α in (6) by ϕ and θ, given by equations (10) and (11). At $\alpha = 0$ the result simplifies to

$$\phi^4 + 2\theta\phi^3 + (\theta^2 - 1)\,\phi^2 = 0,$$

so that

$$\phi = 0, \quad 0, \quad -\theta \pm 1,$$

where the last two correspond to gravity waves. One of the zero roots corresponds to the potentially unstable mode; thus, by setting

$$\phi = \epsilon = \text{small}$$

and neglecting higher powers of ϵ and α, it is found that

$$\epsilon^2[\theta^2 - 1] - 2\theta\alpha\epsilon - [\theta^2 + \rho_b^{-1} - 1]\,\alpha = 0$$

(anticipating that $\theta^2 + \rho_b^{-1} - 1$ will be of order α in the region of interest). Therefore

$$\epsilon = \frac{\theta\alpha \pm \{\theta^2\alpha^2 + (\theta^2 - 1)\,[\theta^2 + \rho_b^{-1} - 1]\,\alpha\}^{\frac{1}{2}}}{\theta^2 - 1}$$

and thus the neutral stability curve is given for small α by

$$\alpha = (\theta^{-2} - 1)\,(\theta^2 + \rho_b^{-1} - 1). \tag{12}$$

This is found to correspond closely to the numerical results for $\alpha \leqslant 0{\cdot}3$. In particular, (12) shows that at $\alpha = 0$ the neutral stability point occurs at

$$\theta = (1 - \rho_b^{-1})^{\frac{1}{2}}.$$

3. Shear-layer profile calculations and results

The second problem considered, which perhaps corresponds more closely to situations experienced in nature, is that of small disturbances superimposed on the flow of figure 1 (*c*). The analysis can be carried out in the same fashion as in the preceding problem, i.e. by defining a separate potential for each layer and

† The referee has kindly pointed out the following argument to explain this situation: in the absence of the current U the dimensional surface wave speed is

$$v_1 = \left(\frac{gh}{\alpha}\right)^{\frac{1}{2}}$$

and similarly the speed of a wave at the lower interface is

$$v_2 = \left(\frac{gh}{\alpha}\right)^{\frac{1}{2}} \left[\frac{(\rho_b - 1)\tanh\alpha}{\rho_b + \tanh\alpha}\right]^{\frac{1}{2}}$$

(these may be derived as a special case of above results by substituting $v = Uc$ in (6), and then setting $U = 0$). Thus θ is the ratio of U to the surface wave speed v_1. However, since the instability at short wavelengths is principally associated with an internal wave, it may be more reasonable to plot results against the ordinate U/v_2, i.e. to compare U to the speed of an internal wave. And indeed, one find that U/v_2 steadily increases on the neutral stability curve as α is decreased.

matching appropriately at interfaces;† however, we now prefer to follow a more general formulation.

If we neglect viscosity and consider only small two-dimensional disturbances, the equations of motion are, in terms of the dimensionless variables of equations (1),

$$\left.\begin{aligned} u_{,t}+V(y)\,u_{,x}+V'(y)\,v+\frac{p_{,x}}{\rho_1}&=0,\\ v_{,t}+V(y)\,v_{,x}+\frac{p_{,y}}{\rho_1}&=-G,\end{aligned}\right\} \tag{13}$$

where quadratic terms in small quantities have been neglected, and total density has been denoted by ρ_1 in order to reserve the symbol ρ for the unperturbed density. The pressure is now eliminated by the usual process of cross-differentiation and subtraction (multiplying by ρ_1, and taking the curl of the vector equation (13)).

Now for the problems of interest it is appropriate to take

$$\rho_1=\rho(y)+\rho'(y)\,\sigma\,e^{i\alpha(x-ct)}; \tag{14}$$

thus the unperturbed density is a function only of y, and the perturbation in density, caused by the perturbation velocity, is taken proportional to $\rho'(y)$, and with the same x and t dependence that will be assumed for the perturbation velocities. The incompressibility condition $D\rho_1/Dt=0$ then implies that

$$\sigma=\frac{-v}{i\alpha(V(y)-c)\,e^{i\alpha(x-ct)}},$$

which renders (14) kinematically compatible with the perturbation velocities. Using (14) to evaluate $\rho_{1,x}$ and $\rho_{1,y}$, and again neglecting terms that are quadratic in small quantities, we have then

$$\rho'u_{,t}+\rho u_{,ty}+\rho' Vu_{,x}+\rho Vu_{,xy}+\rho' V'v+\rho V''v-\rho v_{,tx}-\rho Vv_{,xx}=-\frac{G\rho' v}{V-c}.$$

We now introduce a stream function Ψ, such that $(u,v)=(\Psi_{,y};-\Psi_{,x})$, thereby satisfying the continuity equation, and we assume Ψ to be of the form

$$\Psi=\phi(y)\,e^{i\alpha(x-ct)}.$$

The resulting equation in $\phi(y)$ may be written

$$\left[\rho W^2\left(\frac{\phi}{W}\right)'\right]'-\alpha^2W\rho\phi=\frac{G\rho'\phi}{W},\quad W=W(y)=V(y)-c. \tag{15}$$

This equation is related to the Orr–Sommerfeld equation (Lin 1955), the situation having been simplified by neglecting viscosity but complicated by allowing for a variable density.

Equation (15) is meaningless at points such as $y=0$ where V'' or ρ' do not exist, and matching conditions must be derived for such points. Rewriting (15) as

$$\left[\rho\left(W^2\left(\frac{\phi}{W}\right)'-G\frac{\phi}{W}\right)\right]'=-\rho G\left(\frac{\phi}{W}\right)'+\alpha^2\rho W\phi$$

† Such an analysis was indeed used when this paper was originally submitted. The following more modern derivation was substituted at the suggestion of the referee; it is preferable in that it involves less algebra, and moreover is of much more general applicability. Both approaches of course yield the same eigenvalue equation ((18) below).

and applying the operator

$$\lim_{\epsilon\to 0}\int_{-\epsilon}^{\epsilon}\{\qquad\}dy,$$

we see that the contents of the square bracket must be continuous at such points. A repetition of this argument shows that ϕ/W must likewise be continuous, so the required matching conditions are

$$\rho\left(W^2\left(\frac{\phi}{W}\right)'-G\frac{\phi}{W}\right)\quad\text{and}\quad\frac{\phi}{W}\quad\text{continuous.}\tag{16}$$

Having thus formulated the problem in general, we now consider the special case of the shear-layer profile (figure 1 (*c*)). Equation (15) reduces to

$$\phi''-\alpha^2\phi=0$$

in the layers of constant ρ and W', and we can write the solution as

$$\phi=a_1e^{-\alpha|y|}+a_2e^{-\alpha|y-1|},\tag{17}$$

where the second of conditions (16) has been met, and ϕ has been required to remain bounded as $y\to-\infty$. Two matching conditions remain to be satisfied, namely that the first quantity in (16) be continuous at $y=0$ and at $y=1$. This yields two homogeneous equations in a_1 and a_2, and the determinant must be zero for a non-trivial solution, giving the eigenvalue equation

$$\left[(c-1)^2+\frac{(c-1)}{\alpha}-\frac{G}{\alpha}\right]\left[(\rho_b+1)c^2-\frac{c}{\alpha}-\frac{G}{\alpha}(\rho_b-1)\right]$$
$$=e^{-2\alpha}\left[(c-1)^2-\frac{(c-1)}{\alpha}+\frac{G}{\alpha}\right]\left[(1-\rho_b)c^2+\frac{c}{\alpha}+\frac{G}{\alpha}(\rho_b-1)\right].\tag{18}$$

Roots of this quartic were extracted numerically, using the quadratic factor method (Kunz 1957). Again either no root or one root was found to have positive imaginary part and hence to correspond to an unstable disturbance mode. The results are shown in figures 2 (*a*) and 2 (*b*).

Analytic results of some interest are available for large α. Again expanding c as a series in $e^{-2\alpha}$ as in (7), we find that

$$c_0=\left\{\begin{array}{c}1-\dfrac{1}{2\alpha}[1\pm\{1+4\alpha G\}^{\frac{1}{2}}],\\[2ex]\dfrac{1}{2\alpha(\rho_b+1)}[1\pm\{1+4(\rho_b^2-1)G\alpha\}^{\frac{1}{2}}].\end{array}\right\}\tag{19}$$

The expressions whose roots are taken are intrinsically positive, so to this degree of approximation complex eigenvalues are not found (the correction $c_2e^{-2\alpha}$ is required to yield a complex approximation). However, double roots can exist, when the first and third of the values (19) are equal, i.e. if

$$(\rho_b+1)[2\alpha-1-\{1+4\alpha G\}^{\frac{1}{2}}]=1+\{1+4(\rho_b^2-1)G\alpha\}^{\frac{1}{2}}.\tag{20}$$

This is a line in the $(\alpha, G^{-\frac{1}{2}})$-plane, which appears as the long thin tail at large α in figures 2 (*a*) and 2 (*b*); inclusion of the $e^{-2\alpha}$ terms opens this line up into a region,

very narrow at large α, where a complex conjugate pair of roots exists, with imaginary part exponentially small in α. Equation (20) gives the location of this tail accurately for $\alpha \geqslant 3$. If $\rho_b = 1$, (20) reduces to

$$G = \alpha - 2 + \frac{3}{4\alpha},$$

with similar results for ρ_b near unity. At large α, the curve is asymptotically

$$G \sim \alpha\left[1 + \left\{\frac{\rho_b - 1}{\rho_b + 1}\right\}^{\frac{1}{2}}\right]^{-2}.$$

(Another locus of double roots is obtained by equating the first and fourth roots of (19); however, such double roots are found to be split into a pair of real roots by inclusion of the $e^{-2\alpha}$ terms.)

4. Discussion of shear-layer profile results

Figure 2 (*a*) shows the neutral stability curve in the $(G^{-\frac{1}{2}} = U/(gh)^{\frac{1}{2}}, \alpha)$-plane; points in the enclosed region correspond to unstable disturbance modes. Consider what happens as one moves along a horizontal (G = constant) line in this plane. This corresponds to holding the physical situation constant (U, h, etc., fixed) and increasing the disturbance wave-number α/h, i.e. decreasing the wavelength $\lambda = 2\pi h/\alpha$. At low α the situation is stable, because of the presence of the upper air-water interface. Then as the neutral stability curve is crossed it becomes unstable, due to the phenomenon called Helmholtz instability. The discontinuous profile remains unstable, but the shear-layer profile exhibits a return to stability and the neutral stability curve is crossed a second time; thus only a finite band of wave-numbers are unstable. This agrees with other results (Lin 1955; Esch 1957), which show that high wave-number disturbances, which have small wavelength and therefore can be considered to be localized within a small region in the y-direction, are stable in simple shear flow (Couette flow) or in the neighbourhood of a discontinuity in derivative such as that of the shear-layer profile.

Figure 2 (*b*) merely repeats the same information in terms of the reciprocal vertical co-ordinate $G^{\frac{1}{2}} = (gh)^{\frac{1}{2}}/U$, to show more clearly the situation at small G. In particular the shear-layer neutral stability curve intersects the $G = 0$ axis at about $\alpha = 1{\cdot}8$ for density ratios near unity, so that all wave-numbers $\alpha \leqslant 1{\cdot}8$ are unstable at $G = 0$.

Figures 4 (*a*) and 4 (*b*) show growth rates as a function of $G^{-\frac{1}{2}}$ for various values of α, and correspond to traverses along vertical lines in figure 2 (*a*). In figure 4 (*a*) values of ρ_b less than one are included, and are seen to result in unstable disturbances at and near $U/(gh)^{\frac{1}{2}} = 0$. This effect, called Taylor instability, is strongly dependent on ρ_b, and disappears when $\rho_b \geqslant 1$, i.e. when the situation is statically stable.

The upper region of instability, however, corresponds to instability of the Helmholtz type, and remains present for $\rho_b > 1$, being in fact surprisingly insensitive to changes of ρ_b. An increase in ρ_b pushes this region to slightly higher values of $G^{-\frac{1}{2}}$ (see figures 4 (*a*) and 4 (*b*)), and thus has a slight stabilizing influence,

but so little that the unstable region shown in figure 2 for $\rho_b = 1{\cdot}02$ is approximately correct for all density ratios in the range $1{\cdot}00 \leqslant \rho_b \leqslant 1{\cdot}06$. The physical conclusion indicated is that the stabilizing influence of the density difference at the lower interface is relatively unimportant. This is in striking contrast to the discontinuous profile, where the influence of ρ_b is of essential importance, and all stability is lost if $\rho_b \leqslant 1$.

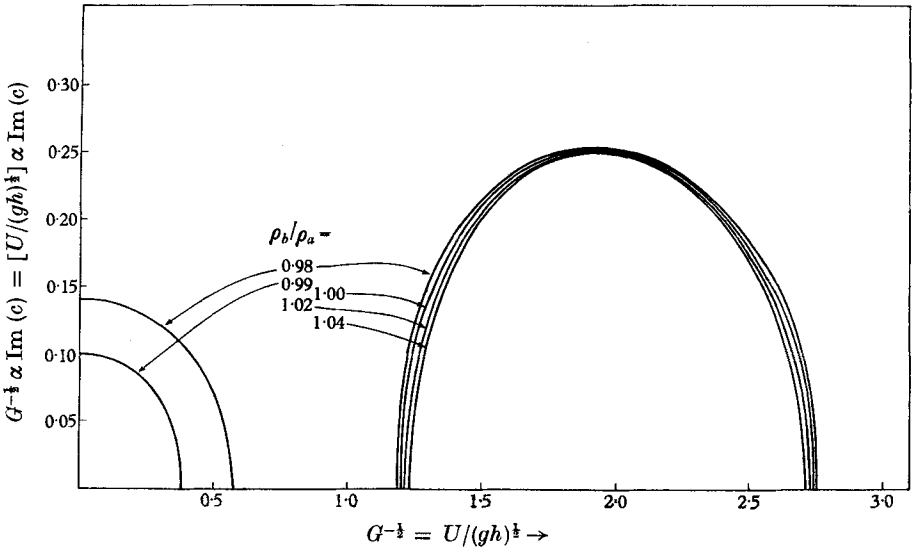

FIGURE 4*a*. Growth-rate curves for the shear-layer profile with $\alpha = 2{\cdot}0$, as a function of the forcing parameter $G^{-\frac{1}{2}} = U/(gh)^{\frac{1}{2}}$. The dimensional growth-rate is $(\alpha U/h)\operatorname{Im}(c)$; this has been multiplied by $(h/g)^{\frac{1}{2}}$ in order to present results in dimensionless form.

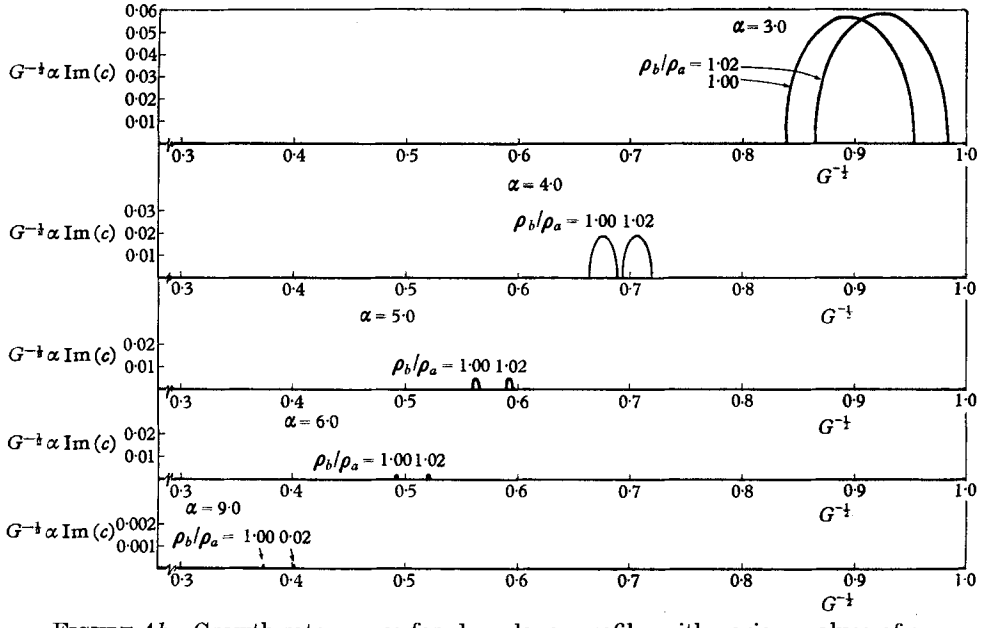

FIGURE 4*b*. Growth-rate curves for shear-layer profile, with various values of α.

At first sight figure 4 (*a*) might seem to indicate that increasing U above zero, i.e. introducing the shearing current, might actually have a stabilizing influence, until it is remembered that disturbances of all wave-numbers must be considered. An increase in U results in lowering the wave-number and increasing the growth rate of the most unstable disturbance.

Now let us consider the question of a critical stream velocity, i.e. a value of U below which unstable disturbances do not occur at any wavelength. The unstable region has been seen to have a thin tail that extends to large α and small $G^{-\frac{1}{2}}$ in an exponentially decreasing manner. Several justifications can be advanced for cutting off this tail at some point. At large α the growth rates become negligibly small (see figure 4 (*b*)); furthermore, the disturbances in question have short wavelength, and thus do not result in real mixing between the moving and still layers of fluid. But these arguments are probably unnecessary, as the inclusion of viscosity in the analysis would probably suffice to remove the instability; it is well known (Lamb 1945; Bellman & Pennington 1954) that the stabilizing effects of viscosity increase with disturbance wave-number, because the amount of shearing motion involved in a sinusoidal disturbance increases as the wavelength decreases.

Looking at figure 4 (*b*) then, a cut-off somewhere in the region $4 < \alpha < 6$ might be anticipated. Certainly the unstable disturbances at $\alpha = 9$ will be unimportant, their growth rate being a factor of 10,000 less than those at $\alpha = 2$. If this reasoning is correct, we can deduce (see figure 2) a critical stream velocity, given by

$$\text{critical } G^{-\frac{1}{2}} = U/(gh)^{\frac{1}{2}} \approx 0{\cdot}5 \text{ to } 0{\cdot}7. \tag{21}$$

For values of $U/(gh)^{\frac{1}{2}}$ below this we anticipate that there will be no important unstable disturbances, and the flow itself can therefore be called stable. As $U/(gh)^{\frac{1}{2}}$ is increased, the first wave-numbers to become unstable are in the neighbourhood of $\alpha = 2\pi h/\lambda = 4$ to 6, so that the first disturbances which may be expected to appear have

$$\text{critical } \lambda \approx h \text{ to } \tfrac{3}{2}h. \tag{22}$$

At higher values of $U/(gh)^{\frac{1}{2}}$ more violent disturbances of a larger scale are predicted.

Even though, as we have argued, the shear-layer instability found at large α almost certainly does not correspond to a real physical instability, it is an intriguing result, and it may be of interest to examine the nature of such disturbance modes. We see from (17) that a_1 and a_2 are the amplitudes of disturbance components centred at $y = 0$ and $y = 1$, i.e. at the lower and upper interfaces respectively. In one sample unstable case, given by

$$\alpha = 5, \quad \rho_b = 1{\cdot}02, \quad U/(gh)^{\frac{1}{2}} = 0{\cdot}593,$$

the relative amplitude of the two components is given by

$$a_1/a_2 = -0{\cdot}012 - (0{\cdot}331)\,i,$$

so that

$$\phi(y) = a[-(0{\cdot}012 + i\,0{\cdot}331)\,e^{-\alpha|y|} + e^{-\alpha|y-1|}].$$

As $\rho_b \to 1$ the lower interface component disappears, i.e. $|a_1|/|a_2| \to 0$, but even for ρ_b only slightly removed from 1 (as in the above example) the disturbance

has a large amplitude at the lower interface. This situation holds at larger values of α, as may be shown by an approximate analysis valid at large α. Thus, even when α is large, so that the interfaces are separated by many wavelengths, we have a situation in which a surface wave at $y = 1$ and an internal wave at $y = 0$ interact in such a manner that energy is extracted, at a very small rate, from the steady flow.

5. Comparison with experimental results

A small glass-walled flume was constructed, with width 3 in., depth $2\frac{3}{4}$ in. and effective length 2 ft. Various amounts of salt were dissolved in a 2 in. deep layer of water in the flume, to provide various density ratios, and ink was mixed in. After the layer had come to rest a stream of tap water was run over the top, at gradually increasing speed, passing first through a 1 ft. section containing calming screens and a dam with sloping approach.

In this rather crude apparatus steady velocity profiles very like figure 1 (*a*) could be achieved (as judged by observation of particles suspended in the water), with layer thicknesses 1–3 cm; velocities from 0 to 12 cm/sec could be achieved. Flows, however, were far from two-dimensional, due to the difficulty in obtaining sufficiently good inlet conditions and to the effects of the side walls of the flume.

After initial small disturbances had quietened down, observation from the side showed a beautifully plane interface between inky water and clear water, the inky region below being completely motionless. Observation from above revealed that the velocity of the upper layer varied across the flume in a somewhat irregular manner. As the velocity was increased, a definite point was reached at which the plane interface began to be gently displaced by disturbances with a definite wavelength. At higher velocities the disturbances became rapidly more violent, soon mixing the two layers.

The measured critical values of $G^{-\frac{1}{2}}$, i.e. values at the onset of disturbances, were about 0·1 or 0·2, and the initial disturbances were observed to have wavelengths in the neighbourhood of $2h$. The uncertainty of these measurements was not due to any difficulty in identifying the point at which disturbances began, but rather to the difficulty of measuring U and h (which varied somewhat along the test section), and eliminating the effects of poor inlet conditions.

The predicted insensitivity of the phenomenon to density ratio was clearly observed, the behaviour of the experiment being much the same whether one or twenty spoonfuls of salt were dissolved in the lower fluid. Only a very small density difference was necessary to allow the steady flow to become established (steady flows of this type are of course impossible without some density difference, because of the effects of viscosity).

The Reynolds number R was always above 1000 at the onset of instability; furthermore, αR was always above 1000 for the disturbances of interest. Consequently we can anticipate that viscosity is important mainly through its effect on the steady-flow profile, and that the errors caused by neglect of viscous terms in the fluid equations for the disturbance are small (see remark in introduction).

The measured critical wavelengths agree fairly well with the values predicted

by the shear-layer analysis, equation (22). However, the measured critical values of $G^{-\frac{1}{2}}$, 0·1–0·2, are significantly less than the predicted value (21). The imperfect inlet conditions and three-dimensional character of the flow explain part of this difference; such difficulties are in part not the result of crude experimental technique but are inherent in flume experiments. Moreover, the experimental and 'shear-layer' profiles are different, and should have somewhat different critical values of $G^{-\frac{1}{2}}$. Since the steepness of the slope (amount of vorticity) is probably the important profile characteristic, we might expect the profile of figure 1 (*a*) to have stability characteristics bracketed by those of the 'shear-layer' and the 'discontinuous' profiles, figures 1 (*b*) and 1 (*c*), and thus to have a neutral stability curve on figure 2 which lies between the two curves shown. The experimental evidence supports this prediction.

6. Conclusions

In the problem considered, where a layer of water flows over a dead region, the stability or instability of the motion can be explained by the classical-analysis methods of Rayleigh. The important parameter is $U/(gh)^{\frac{1}{2}}$, where U is current velocity and h is shear-layer width. This parameter has a critical value, probably between 0·2 and 0·7, and stable flows can persist if it is below this critical value. At the onset of instability, disturbances of wavelength about h or $2h$ are predicted; for higher values of $U/(gh)^{\frac{1}{2}}$ more violent disturbances of longer wavelength can be expected.

There is reason to believe that the neutral stability curves given in figures 2 (*a*) and 2 (*b*) for the two idealized profiles shown in figures 1 (*b*) and 1 (*c*) represent bounds for the neutral stability curve corresponding to a 'real' profile, such as figure 1 (*a*).

The insensitivity of the phenomenon to the difference between the densities of the two regions is of some practical interest. A steady flow of the type considered can be established with only a very small density difference, such as results from minor temperature variations. Therefore such flow patterns may tend to form spontaneously even in a nearly homogeneous fluid, whenever the resulting values of $U/(gh)^{\frac{1}{2}}$ are below the critical values.

This work was partially supported by the Office of Naval Research, under contract N 5 ori-07634. Computer time was paid for by National Science Foundation grant No. NSF-G-4611.

REFERENCES

BELLMAN, R. & PENNINGTON, R. H. 1954 Effects of surface tension and viscosity on Taylor instability. *Quart. appl. Math.* **12**, 151.

BJERKNES, V., BJERKNES, J., SOLBERG, H. & BERGERON, T. 1933 *Physikalische Hydrodynamik.* Berlin: Springer.

DRAZIN, P. G. 1958 The stability of a shear layer in an unbounded heterogeneous inviscid fluid. *J. Fluid Mech.* **4**, 214.

ESCH, R. E. 1957 The instability of a shear layer between two parallel streams. *J. Fluid Mech.* **3**, 289.

GODSKE, C. L., BERGERON, T., BJERKNES, J. & BUNDGAARD, R. C. 1957 *Dynamic Meteorology and Weather Forecasting*. Boston, American Meteorological Society, and Washington, Carnegie Institute of Washington.

GOLDSTEIN, S. 1931 On the stability of superposed streams of fluids of different densities. *Proc. Roy. Soc.* A, **132**, 524.

KUNZ, K. S. 1957 *Numerical Analysis*. New York: McGraw-Hill.

LAMB, H. 1945 *Hydrodynamics*. Cambridge University Press.

LIN, C. C. 1955 *Theory of Hydrodynamic Stability*. Cambridge University Press.

MENKES, J. 1959 On the stability of a shear layer. *J. Fluid Mech.* **6**, 518.

RAYLEIGH, LORD 1945 *Theory of Sound*. New York: Dover.

TAYLOR, G. I. 1931 Effect of variation in density on the stability of superposed streams of fluid. *Proc. Roy. Soc.* A, **132**, 499.